Measurement of Λ and $\overline{\Lambda}$ Particles in Au + Au Collisions at $\sqrt{s_{NN}} = 130$ GeV

K. Adcox,[40] S. S. Adler,[3] N. N. Ajitanand,[27] Y. Akiba,[14] J. Alexander,[27] L. Aphecetche,[34] Y. Arai,[14] S. H. Aronson,[3] R. Averbeck,[28] T. C. Awes,[29] K. N. Barish,[5] P. D. Barnes,[19] J. Barrette,[21] B. Bassalleck,[25] S. Bathe,[22] V. Baublis,[30] A. Bazilevsky,[12,32] S. Belikov,[12,13] F. G. Bellaiche,[29] S. T. Belyaev,[16] M. J. Bennett,[19] Y. Berdnikov,[35] S. Botelho,[33] M. L. Brooks,[19] D. S. Brown,[26] N. Bruner,[25] D. Bucher,[22] H. Buesching,[22] V. Bumazhnov,[12] G. Bunce,[3,32] J. Burward-Hoy,[28] S. Butsyk,[28,30] T. A. Carey,[19] P. Chand,[2] J. Chang,[5] W. C. Chang,[1] L. L. Chavez,[25] S. Chernichenko,[12] C. Y. Chi,[8] J. Chiba,[14] M. Chiu,[8] R. K. Choudhury,[2] T. Christ,[28] T. Chujo,[3,39] M. S. Chung,[15,19] P. Chung,[27] V. Cianciolo,[29] B. A. Cole,[8] D. G. D'Enterria,[34] G. David,[3] H. Delagrange,[34] A. Denisov,[12] A. Deshpande,[32] E. J. Desmond,[3] O. Dietzsch,[33] B. V. Dinesh,[2] A. Drees,[28] A. Durum,[12] D. Dutta,[2] K. Ebisu,[24] Y. V. Efremenko,[29] K. El Chenawi,[40] H. En'yo,[17,31] S. Esumi,[39] L. Ewell,[3] T. Ferdousi,[5] D. E. Fields,[25] S. L. Fokin,[16] Z. Fraenkel,[42] A. Franz,[3] A. D. Frawley,[9] S. -Y. Fung,[5] S. Garpman,[20,*] T. K. Ghosh,[40] A. Glenn,[36] A. L. Godoi,[33] Y. Goto,[32] S. V. Greene,[40] M. Grosse Perdekamp,[32] S. K. Gupta,[2] W. Guryn,[3] H. -Å. Gustafsson,[20] J. S. Haggerty,[3] H. Hamagaki,[7] A. G. Hansen,[19] H. Hara,[24] E. P. Hartouni,[18] R. Hayano,[38] N. Hayashi,[31] X. He,[10] T. K. Hemmick,[28] J. M. Heuser,[28] M. Hibino,[41] J. C. Hill,[13] D. S. Ho,[43] K. Homma,[11] B. Hong,[15] A. Hoover,[26] T. Ichihara,[31,32] K. Imai,[17,31] M. S. Ippolitov,[16] M. Ishihara,[31,32] B. V. Jacak,[28,32] W. Y. Jang,[15] J. Jia,[28] B. M. Johnson,[3] S. C. Johnson,[18,28] K. S. Joo,[23] S. Kametani,[41] J. H. Kang,[43] M. Kann,[30] S. S. Kapoor,[2] S. Kelly,[8] B. Khachaturov,[42] A. Khanzadeev,[30] J. Kikuchi,[41] D. J. Kim,[43] H. J. Kim,[43] S. Y. Kim,[43] Y. G. Kim,[43] W. W. Kinnison,[19] E. Kistenev,[3] A. Kiyomichi,[39] C. Klein-Boesing,[22] S. Klinksiek,[25] L. Kochenda,[30] V. Kochetkov,[12] D. Koehler,[25] T. Kohama,[11] D. Kotchetkov,[5] A. Kozlov,[42] P. J. Kroon,[3] K. Kurita,[31,32] M. J. Kweon,[15] Y. Kwon,[43] G. S. Kyle,[26] R. Lacey,[27] J. G. Lajoie,[13] J. Lauret,[27] A. Lebedev,[13,16] D. M. Lee,[19] M. J. Leitch,[19] X. H. Li,[5] Z. Li,[6,31] D. J. Lim,[43] M. X. Liu,[19] X. Liu,[6] Z. Liu,[6] C. F. Maguire,[40] J. Mahon,[3] Y. I. Makdisi,[3] V. I. Manko,[16] Y. Mao,[6,31] S. K. Mark,[21] S. Markacs,[8] G. Martinez,[34] M. D. Marx,[28] A. Masaike,[17] F. Matathias,[28] T. Matsumoto,[7,41] P. L. McGaughey,[19] E. Melnikov,[12] M. Merschmeyer,[22] F. Messer,[28] M. Messer,[3] Y. Miake,[39] T. E. Miller,[40] A. Milov,[42] S. Mioduszewski,[3,36] R. E. Mischke,[19] G. C. Mishra,[10] J. T. Mitchell,[3] A. K. Mohanty,[2] D. P. Morrison,[3] J. M. Moss,[19] F. Mühlbacher,[28] D. Mukhopadhyay,[42] M. Muniruzzaman,[5] J. Murata,[31] S. Nagamiya,[14] Y. Nagasaka,[24] J. L. Nagle,[8] Y. Nakada,[17] B. K. Nandi,[5] J. Newby,[36] L. Nikkinen,[21] P. Nilsson,[20] S. Nishimura,[7] A. S. Nyanin,[16] J. Nystrand,[20] E. O'Brien,[3] C. A. Ogilvie,[13] H. Ohnishi,[3,11] I. D. Ojha,[4,40] M. Ono,[39] V. Onuchin,[12] A. Oskarsson,[20] L. Österman,[20] I. Otterlund,[20] K. Oyama,[7,38] L. Paffrath,[3,*] D. Pal,[42] A. P. T. Palounek,[19] V. S. Pantuev,[28] V. Papavassiliou,[26] S. F. Pate,[26] T. Peitzmann,[22] A. N. Petridis,[13] C. Pinkenburg,[3,27] R. P. Pisani,[3] P. Pitukhin,[12] F. Plasil,[29] M. Pollack,[28,36] K. Pope,[36] M. L. Purschke,[3] I. Ravinovich,[42] K. F. Read,[29,36] K. Reygers,[22] V. Riabov,[30,35] Y. Riabov,[30] M. Rosati,[13] A. A. Rose,[40] S. S. Ryu,[43] N. Saito,[31,32] A. Sakaguchi,[11] T. Sakaguchi,[7,41] H. Sako,[39] T. Sakuma,[31,37] V. Samsonov,[30] T. C. Sangster,[18] R. Santo,[22] H. D. Sato,[17,31] S. Sato,[39] S. Sawada,[14] B. R. Schlei,[19] Y. Schutz,[34] V. Semenov,[12] R. Seto,[5] T. K. Shea,[3] I. Shein,[12] T. -A. Shibata,[31,37] K. Shigaki,[14] T. Shiina,[19] Y. H. Shin,[43] I. G. Sibiriak,[16] D. Silvermyr,[20] K. S. Sim,[15] J. Simon-Gillo,[19] C. P. Singh,[4] V. Singh,[4] M. Sivertz,[3] A. Soldatov,[12] R. A. Soltz,[18] S. Sorensen,[29,36] P. W. Stankus,[29] N. Starinsky,[21] P. Steinberg,[8] E. Stenlund,[20] A. Ster,[44] S. P. Stoll,[3] M. Sugioka,[31,37] T. Sugitate,[11] J. P. Sullivan,[19] Y. Sumi,[11] Z. Sun,[6] M. Suzuki,[39] E. M. Takagui,[33] A. Taketani,[31] M. Tamai,[41] K. H. Tanaka,[14] Y. Tanaka,[24] E. Taniguchi,[31,37] M. J. Tannenbaum,[3] J. Thomas,[28] J. H. Thomas,[18] T. L. Thomas,[25] W. Tian,[6,36] J. Tojo,[17,31] H. Torii,[17,31] R. S. Towell,[19] I. Tserruya,[42] H. Tsuruoka,[39] A. A. Tsvetkov,[16] S. K. Tuli,[4] H. Tydesjö,[20] N. Tyurin,[12] T. Ushiroda,[24] H. W. van Hecke,[19] C. Velissaris,[26] J. Velkovska,[28] M. Velkovsky,[28] A. A. Vinogradov,[16] M. A. Volkov,[16] A. Vorobyov,[30] E. Vznuzdaev,[30] H. Wang,[5] Y. Watanabe,[31,32] S. N. White,[3] C. Witzig,[3] F. K. Wohn,[13] C. L. Woody,[3] W. Xie,[5,42] K. Yagi,[39] S. Yokkaichi,[31] G. R. Young,[29] I. E. Yushmanov,[16] W. A. Zajc,[8] Z. Zhang,[28] S. Zhou,[6] and S. Zhou[42]

(PHENIX Collaboration)

[1]*Institute of Physics, Academia Sinica, Taipei 11529, Taiwan*
[2]*Bhabha Atomic Research Centre, Bombay 400 085, India*
[3]*Brookhaven National Laboratory, Upton, New York 11973-5000*
[4]*Department of Physics, Banaras Hindu University, Varanasi 221005, India*
[5]*University of California–Riverside, Riverside, California 92521*
[6]*China Institute of Atomic Energy (CIAE), Beijing, People's Republic of China*
[7]*Center for Nuclear Study, Graduate School of Science, University of Tokyo, 7-3-1 Hongo, Bunkyo, Tokyo 113-0033, Japan*
[8]*Columbia University, New York, New York 10027 and Nevis Laboratories, Irvington, New York 10533*

 0031-9007/02/89(9)/092302(6)$20.00

[9]*Florida State University, Tallahassee, Florida 32306*
[10]*Georgia State University, Atlanta, Georgia 30303*
[11]*Hiroshima University, Kagamiyama, Higashi-Hiroshima 739-8526, Japan*
[12]*Institute for High Energy Physics (IHEP), Protvino, Russia*
[13]*Iowa State University, Ames, Iowa 50011*
[14]*KEK, High Energy Accelerator Research Organization, Tsukuba-shi, Ibaraki-ken 305-0801, Japan*
[15]*Korea University, Seoul, 136-701, Korea*
[16]*Russian Research Center "Kurchatov Institute," Moscow, Russia*
[17]*Kyoto University, Kyoto 606, Japan*
[18]*Lawrence Livermore National Laboratory, Livermore, California 94550*
[19]*Los Alamos National Laboratory, Los Alamos, New Mexico 87545*
[20]*Department of Physics, Lund University, Box 118, SE-221 00 Lund, Sweden*
[21]*McGill University, Montreal, Quebec H3A 2T8, Canada*
[22]*Institut für Kernphysik, University of Münster, D-48149 Münster, Germany*
[23]*Myongji University, Yongin, Kyonggido 449-728, Korea*
[24]*Nagasaki Institute of Applied Science, Nagasaki-shi, Nagasaki 851-0193, Japan*
[25]*University of New Mexico, Albuquerque, New Mexico 87131*
[26]*New Mexico State University, Las Cruces, New Mexico 88003*
[27]*Chemistry Department, State University of New York–Stony Brook, Stony Brook, New York 11794*
[28]*Department of Physics and Astronomy, State University of New York–Stony Brook, Stony Brook, New York 11794*
[29]*Oak Ridge National Laboratory, Oak Ridge, Tennessee 37831*
[30]*PNPI, Petersburg Nuclear Physics Institute, Gatchina, Russia*
[31]*RIKEN (The Institute of Physical and Chemical Research), Wako, Saitama 351-0198, Japan*
[32]*RIKEN BNL Research Center, Brookhaven National Laboratory, Upton, New York 11973-5000*
[33]*Universidade de São Paulo, Instituto de Física, Caixa Postal 66318, São Paulo CEP05315-970, Brazil*
[34]*SUBATECH (Ecole des Mines de Nantes, IN2P3/CNRS, Universite de Nantes), BP 20722-44307, Nantes Cedex 3, France*
[35]*St. Petersburg State Technical University, St. Petersburg, Russia*
[36]*University of Tennessee, Knoxville, Tennessee 37996*
[37]*Department of Physics, Tokyo Institute of Technology, Tokyo, 152-8551, Japan*
[38]*University of Tokyo, Tokyo, Japan*
[39]*Institute of Physics, University of Tsukuba, Tsukuba, Ibaraki 305, Japan*
[40]*Vanderbilt University, Nashville, Tennessee 37235*
[41]*Waseda University, Advanced Research Institute for Science and Engineering, 17 Kikui-cho, Shinjuku-ku, Tokyo 162-0044, Japan*
[42]*Weizmann Institute, Rehovot 76100, Israel*
[43]*Yonsei University, IPAP, Seoul 120-749, Korea*
[44]*KFKI Research Institute for Particle and Nuclear Physics (RMKI), Budapest, Hungary*[†]
(Received 17 April 2002; published 12 August 2002)

We present results on the measurement of Λ and $\bar{\Lambda}$ production in Au + Au collisions at $\sqrt{s_{NN}} =$ 130 GeV with the PHENIX detector at the Relativistic Heavy Ion Collider. The transverse momentum spectra were measured for minimum bias and for the 5% most central events. The $\bar{\Lambda}/\Lambda$ ratios are constant as a function of p_T and the number of participants. The measured net Λ density is significantly larger than predicted by models based on hadronic strings (e.g., HIJING) but in approximate agreement with models which include the gluon-junction mechanism.

DOI: 10.1103/PhysRevLett.89.092302 PACS numbers: 25.75.Dw

In this Letter we report on the measurement by the PHENIX experiment at the Relativistic Heavy Ion Collider (RHIC) of the production of Λ and $\bar{\Lambda}$ particles and the ratio $\bar{\Lambda}/\Lambda$ as a function of transverse momentum p_T and centrality in Au + Au collisions at $\sqrt{s_{NN}} =$ 130 GeV. The production of strange baryons and of strange particles in general has been extensively studied in heavy ion collisions at the Alternating Gradient Synchrotron (AGS) and at the Super Proton Synchrotron (SPS) [1] to investigate the flavor composition of nuclear matter at high density and temperature. Furthermore, antibaryon-to-baryon ratios, or alternatively, a net baryon number such as $(\Lambda - \bar{\Lambda})$ at midrapidity provide insight into the baryon transport mechanism in these collisions [2–5]. The systematic study of baryon stopping (transport of baryon number in rapidity space) and hyperon production in proton-proton, proton-nucleus, and nucleus-nucleus collisions has been done over the past decade at the AGS [6,7] and CERN SPS [8–10]. The results have shown a high degree of baryon stopping and enhanced hyperon production in heavy nucleus-nucleus collisions. Clearly the measurement of these quantities at RHIC, at the highest energies so far available in the laboratory, is of great importance for our understanding of the sources of these processes.

The results reported here were obtained using the west arm of the PHENIX spectrometer [11] which covers an angular range of $\Delta\phi = \pi/4$ (during its first year of running) and a pseudorapidity range of $|\eta| < 0.35$. The detectors used were the drift chamber (DC), a set of multiwire proportional chambers with pixel-pad readout (PC1) [12], and a lead-scintillator electromagnetic calorimeter (EMCal) [13]. Signals from two sets of beam-beam counters (BBC) and two zero-degree calorimeters (ZDC) provided a trigger sensitive to $92\% \pm 4\%$ of the 6.8 b total Au + Au cross section [14]. The centrality selection was done using the correlation between the analog responses of the ZDC and BBC [14].

The present analysis is based on 1.3 M minimum-bias events with a vertex position of $|z| < 20$ cm. To reconstruct the Λ and $\bar{\Lambda}$ particles, their weak decays $\Lambda \rightarrow p\pi^-$ and $\bar{\Lambda} \rightarrow \bar{p}\pi^+$ are used. The tracks of the charged particles from the decay of Λ and $\bar{\Lambda}$ are reconstructed using DC and PC1, and their momentum is determined by the DC with a resolution of $\delta p/p \simeq 0.6\% \oplus 3.6\% p$ (GeV/c). Although these tracks do not point back to the primary vertex position (the mean distance of the Λ decay vertex to interaction vertex is $\sim$3.5 cm), their momentum is calculated assuming that they come from the interaction point, hence there is, in general, a shift in the momentum of the reconstructed Λ and $\bar{\Lambda}$ particles. A Monte Carlo (MC) study shows that the difference is of the order 1%–2% over the measured momentum range, within the measured momentum resolution, and thus neglected in the present study. The absolute momentum scale is known to better than 2% [15]. In order to reduce background the tracks are confirmed by requiring a matching hit in the EMCal within $\pm 3\sigma$. For the particle identification of the daughter charged particles the time-of-flight signal of the EMCal with a timing resolution of $\sim$700 ps is used. Using the momentum measured by the DC and the flight time, the particle mass is calculated and a 2σ momentum-dependent cut is applied to the mass-squared distribution to identify protons, antiprotons, and pions. An upper momentum cut of 0.6 and 1.4 GeV/c for pions and protons, respectively, provides clean particle separation. Then each proton is combined with each pion in the same event and the invariant mass is calculated. If Λ or $\bar{\Lambda}$ are produced, a peak appears in the mass distribution on top of a background from random combinations of particles and short lived resonances (Δ and N^*). In order to determine the number of Λ's and $\bar{\Lambda}$'s from such a distribution, an estimation of the background is essential. For this, the mass distribution with combinations of protons and pions from different events with the same centrality class (event mixing) is used. In order to reduce the background, the decay proton energy is required to be within $E_p^{\min} < E_p < E_p^{\max}$, where $E_p^{\min}$ and $E_p^{\max}$ are calculated from the two-body decay kinematics in the Λ center-of-mass system. A similar cut is used for the pions. This cut is particularly effective in reducing the contributions from short-lived resonances and gives an improvement of the signal-to-background ratio by a factor of 2 without affecting the Λ line shape and results in the final value of $S/B = 1/2$ for both Λ and $\bar{\Lambda}$. We obtain $\sim$12000 Λ and $\sim$9000 $\bar{\Lambda}$ particles in the mass range $1.05 < m_{p\pi} < 1.20$ GeV/c^2 with mass resolution $\delta m/m \simeq 2\%$ obtained from a Gaussian fit. The Λ ($\bar{\Lambda}$) peaks vary by less than the mass resolution over the measured p_T range.

Figure 1 shows the invariant mass spectra for the $\Lambda \rightarrow p\pi^-$ and $\bar{\Lambda} \rightarrow \bar{p}\pi^+$. The results represent the primary Λ and $\bar{\Lambda}$ and contributions from the feed-down from heavier hyperons (mainly Σ^0 and Ξ). The reconstructed number of Λ and $\bar{\Lambda}$ particles is corrected for acceptance, pion decay-in-flight, momentum resolution, and reconstruction efficiency. For this, single-particle MC events were generated over the full azimuth ϕ ($0 < \phi < 2\pi$) and one unit of rapidity y ($-0.5 < y < 0.5$). The simulated particles were passed through the entire PHENIX GEANT [16] simulation. The correction function is defined as the ratio of the input (generated) transverse momentum distribution to the p_T distribution of the particles reconstructed in the spectrometer. However, this correction does not take into account the decreasing track reconstruction efficiency due to the high multiplicity environment in more central events. A well-established method to obtain this efficiency drop is the embedding procedure [15]. We use single-particle MC tracks embedded into real events and analyze the merged events with the same analysis code as used for the reconstruction of the data set. The track reconstruction efficiency decreases from 90% for minimum bias to 70%

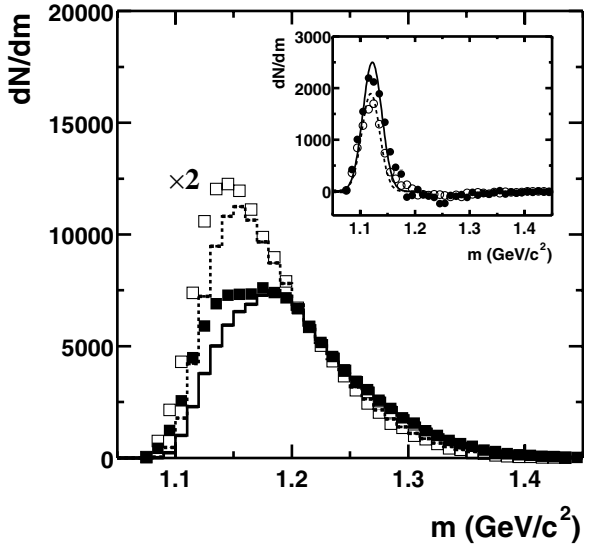

FIG. 1. Invariant mass spectra of $p\pi^-$ (solid squares) and $\bar{p}\pi^+$ (open squares) pairs. The histograms show the background for $p\pi^-$ (solid line) and $\bar{p}\pi^+$ (dashed line). For clarity the $\bar{p}\pi^+$ data are scaled up by a factor of 2. The inset shows the background-subtracted spectra of Λ (solid circles) and $\bar{\Lambda}$ (open circles). The lines are Gaussian fits to the Λ (solid line) and $\bar{\Lambda}$ (dashed line) mass spectra.

for central events, independently of the track p_T. The Σ^0 and Ξ hyperons decay to Λ with a branching ratio of essentially 100%. We have verified, using HIJING, that the kinematic properties (p_T and y distributions) of primary Λ and those produced by Σ^0 and Ξ decay are the same (within a few percent). We conclude that the correction function determined for primary Λ is valid for all Λ. Since there are no reliable data available for the yields of those hyperons at RHIC energies, we cannot quantitatively state the contributions from those heavier hyperons to our Λ production. Therefore, our data include the primordial Λ and $\bar{\Lambda}$, as well as the feed-down from the heavier hyperons.

Using the correction function determined from single-particle MC and multiplicity-dependent track reconstruction efficiency derived from the embedding procedure, we correct the transverse momentum distributions of Λ and $\bar{\Lambda}$. The invariant yields as a function of the transverse momentum p_T for Λ and $\bar{\Lambda}$ are shown in Fig. 2 for minimum-bias events (circles). Over the measured transverse momentum range ($0.4 < p_T < 1.8$ GeV/c), both the Λ and $\bar{\Lambda}$ spectra can be described by a distribution of the form $dN/dp_T^2 \propto p_T e^{-p_T/T}$ as shown in Fig. 2 by the solid line. The total yield dN/dy is obtained by integrating the functional fit from zero to infinity. The fraction of the extrapolated yield is 29%. In the same Fig. 2 we show the invariant yield for the 5% most central events (squares). In Table I the total yields dN/dy together with the average transverse momentum $\langle p_T \rangle$ and the slope parameters T are listed for both minimum bias and for the 5% most central events.

There are several sources which contribute to the systematic uncertainties of the total yield dN/dy and average transverse momentum $\langle p_T \rangle$ determination. One of the sources, the uncertainty in the correction function determination, is found to be 13%. By changing the fitting function used for the yield extrapolation to a pure exponential, we derive a systematic error of $\pm 9\%$. There is also an additional contribution to the systematic error which originates from the combinatorial background subtraction which is 3%. Combining the above uncertainties in quadrature gives a total systematic error in the yield of 16% (see Table I).

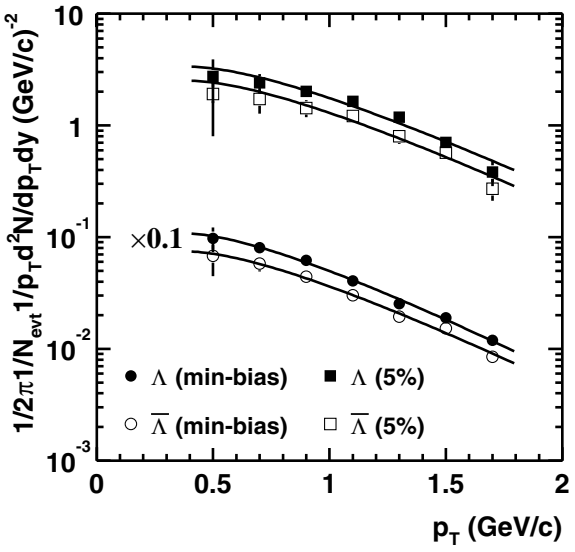

FIG. 2. Transverse momentum spectra of Λ and $\bar{\Lambda}$ for minimum bias and for the 5% most central events. For clarity of presentation the data points for minimum bias are scaled down by a factor of 10.

The $\bar{\Lambda}/\Lambda$ yield ratio determined in the mass window defined above versus p_T is shown in Fig. 3 (top panel). The ratio is constant over the whole p_T range $0.4 < p_T < 1.8$ GeV/c. There is also no significant variation of the $\bar{\Lambda}/\Lambda$ ratio as a function of the number of participants (bottom panel) which is calculated using a Glauber model together with a simulation of the ZDC and BBC responses [14]. The average $\bar{\Lambda}/\Lambda$ ratio is $0.75 \pm 0.09(\text{stat}) \pm 0.17(\text{syst})$. Both the p_T dependence and the integral $\bar{\Lambda}/\Lambda$ ratio are consistent with statistical thermal model calculations [17] at RHIC energies.

The present measurement of the total yield of Λ and $\bar{\Lambda}$ enables us to take the previously reported inclusive p and $\bar{p}$ spectra [18] and construct a feed-down correction for Λ decays. As the Σ yield has not been measured, we do

TABLE I. Inclusive Λ and feed-down corrected proton yields, average transverse momentum (in GeV/c), and slope parameters (in MeV/c) for minimum bias (MB) and for the 5% most central events. The errors listed are statistical. The systematic errors are 17% for the protons and 16% for the Λ.

		Λ	$\bar{\Lambda}$	p	$\bar{p}$
dN/dy	(MB)	4.8 ± 0.3	3.5 ± 0.3	5.4 ± 0.2	3.7 ± 0.2
	(5%)	17.3 ± 1.8	12.7 ± 1.8	19.3 ± 0.6	13.7 ± 0.7
$\langle p_T \rangle$	(MB)	1.06 ± 0.08	1.10 ± 0.12	0.88 ± 0.04	0.91 ± 0.06
	(5%)	1.15 ± 0.15	1.14 ± 0.21	0.95 ± 0.07	1.04 ± 0.12
T	(MB)	355 ± 11	366 ± 13	292 ± 21	304 ± 23
	(5%)	384 ± 16	380 ± 19	319 ± 31	327 ± 34

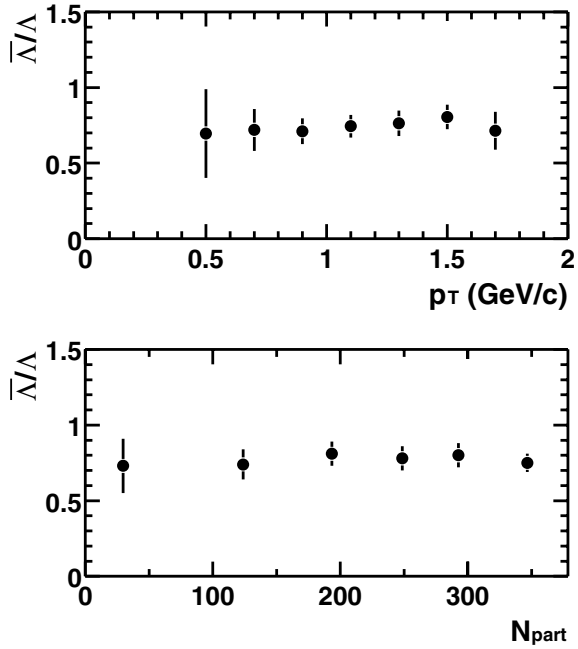

FIG. 3. The ratio $\bar{\Lambda}/\Lambda$ as a function of p_T (top) and as a function of the number of participants (bottom).

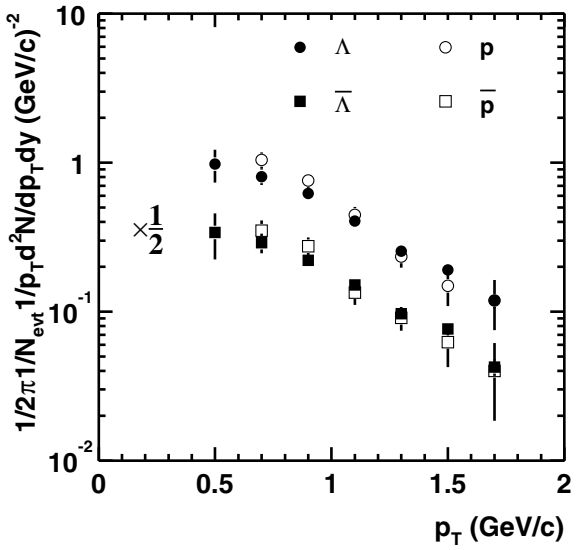

FIG. 4. Spectra of inclusive Λ ($\bar{\Lambda}$) and feed-down corrected protons (antiprotons) for minimum-bias events. The data points for antiprotons and $\bar{\Lambda}$ are scaled down by a factor of 2.

not include feed-down from $\Sigma^{\pm}$ decays, but this is expected to be $<5\%$, based on HIJING calculations. The feed-down corrections were done bin by bin on the proton (antiproton) p_T spectrum by the following method:

$$\frac{dN^p}{dydp_T}(i) = \frac{dN^m}{dydp_T}(i) - \sum_{j=1}^{N_{\text{bins}}} \frac{dN^{\Lambda}}{dydp_T}(j) \times BR \times w(j,i), \tag{1}$$

where $dN^p/dydp_T$ is the total yield of the primary protons, $dN^m/dydp_T$ is the total yield of the measured protons, $dN^{\Lambda}/dydp_T$ is the total yield of the measured Λ, BR is the branching ratio of the Λ decay $\Lambda \rightarrow p\pi^-$, i is the p_T bin number, N_{bins} is the number of bins, and $w(j,i)$ is the fraction of protons from Λ decay from bin number j which fall into the proton bin number i. These fractions were extracted from MC. The feed-down corrected proton and antiproton p_T spectra are shown in Fig. 4. We calculated the total yield, dN/dy, for protons and antiprotons by fitting them to the same distribution as used for the Λ and integrating from zero to infinity. The results for the total yields dN/dy, the average transverse momentum $\langle p_T \rangle$, and the slope parameters T for minimum bias and for the 5% most central events are also listed in Table I. The measured Λ/p and $\bar{\Lambda}/\bar{p}$ ratios after feed-down corrections are found to be $0.89 \pm 0.07(\text{stat}) \pm 0.21(\text{syst})$ and $0.95 \pm 0.09(\text{stat}) \pm 0.22(\text{syst})$.

The net baryon numbers are indicative of the baryon transport mechanism in relativistic heavy ion (RHI) collisions. In Table II we compare our results for minimum bias and for the 5% most central events with the predictions of the HIJING [19] model which assumes that the primary mechanism for baryon transport in RHI is due to quark-diquark hadronic strings. Vance *et al.* [4] implemented a nonperturbative gluon-junction mechanism in a new version of HIJING (called HIJING/B) to explain the enhanced baryon stopping at CERN SPS energies. The predictions of this model are also shown in Table II. For a valid comparison with the experimental data, the HIJING and HIJING/B results for Λ and $\bar{\Lambda}$ also include the feed-down from the heavier hyperons and the results for protons and antiprotons the feed-down from $\Sigma^{\pm}$. Table II shows a clear difference (by a factor of $\sim$4) between HIJING and HIJING/B for the net Λ number, with the HIJING/B predictions in much better agreement, in particular, for the minimum-bias data, where the experimental errors are relatively small. Moreover, HIJING/B rapidity densities for both Λ and $\bar{\Lambda}$ are closer to the experimental values though still below them. The difference between the two models for the net proton number is less obvious and, although the data seem

TABLE II. Total measured and predicted baryon yields for minimum bias (MB) and for the 5% most central events. The errors listed are statistical. The proton yields are corrected for feed-down. The systematic errors are 24% for the protons and 23% for the Λ.

Net baryon number	PHENIX	HIJING	HIJING/B
$(\Lambda - \bar{\Lambda})$ (MB)	1.3 ± 0.4	0.2	0.8
$(p - \bar{p})$ (MB)	1.7 ± 0.3	1.1	1.7
$(\Lambda - \bar{\Lambda})$ (5%)	4.6 ± 2.5	0.8	3.2
$(p - \bar{p})$ (5%)	5.6 ± 0.9	4.7	7.1

to favor HIJING/B, the present accuracy does not allow for a clear preference between the two models.

In conclusion, we have measured the transverse momentum spectra of Λ and $\bar{\Lambda}$ particles in the p_T range $0.4 < p_T < 1.8$ GeV/c in minimum bias and the 5% most central Au + Au collisions at $\sqrt{s_{NN}} = 130$ GeV at RHIC with the PHENIX experiment. The absolute yields of dN/dy, at midrapidity, of Λ hyperons are determined by extrapolating to all values of p_T. The average $\bar{\Lambda}/\Lambda$ ratio is found to be $0.75 \pm 0.09 \pm 0.17$. The ratio is constant over the whole p_T range and there is also no significant variation of the $\bar{\Lambda}/\Lambda$ ratio as a function of the number of participants. Using the measured Λ and $\bar{\Lambda}$ yields, the p and $\bar{p}$ yields corrected for feed-down from Λ decays are determined. The Λ/p and $\bar{\Lambda}/\bar{p}$ ratios after feed-down corrections are found to be $0.89 \pm 0.07 \pm 0.21$ and $0.95 \pm 0.09 \pm 0.22$. The measured net Λ number is substantially larger than predicted by HIJING as already seen at CERN SPS and which may indicate enhanced baryon stopping at RHI energies. The newly available high statistics data at $\sqrt{s_{NN}} = 200$ GeV will allow us to further study baryon transport and strangeness production in RHI collisions.

We thank the staff of the Collider-Accelerator and Physics Departments at BNL for their vital contributions. We acknowledge support from the Department of Energy and NSF (U.S.), MEXT and JSPS (Japan), RAS, RMAE, and RMS (Russia), BMBF, DAAD, and AvH (Germany), VR and KAW (Sweden), MIST and NSERC (Canada), CNPq and FAPESP (Brazil), IN2P3/CNRS (France), DAE and DST (India), KRF and CHEP (Korea), the U.S. CRDF for the FSU, and the US–Israel BSF.

*Deceased.
†Not a participating institution.

[1] *5th International Conference on Strangeness in Quark Matter 2000* [J. Phys. G **27**, 255 (2001)], and references therein.
[2] B. Z. Kopeliovich and B. G. Zakharov, Z. Phys. C **43**, 241 (1989).
[3] D. Kharzeev, Phys. Lett. B **378**, 238 (1996).
[4] S. E. Vance *et al.*, Phys. Lett. B **443**, 45 (1998).
[5] M. Gyulassy and I. Vitev, nucl-th/0104066.
[6] S. Ahmad *et al.*, Phys. Lett. B **382**, 35 (1996).
[7] K. Filimonov *et al.*, Nucl. Phys. **A661**, 198c (1999).
[8] T. Alber *et al.*, Eur. J. Phys. C **2**, 643 (1998).
[9] K. Wolf *et al.*, Phys. Rev. C **57**, 837 (1998).
[10] H. Appelshäuser *et al.*, Phys. Rev. Lett. **82**, 2471 (1999).
[11] PHENIX Collaboration, D. P. Morrison *et al.*, Nucl. Phys. **A638**, 565c (1998).
[12] P. Nilsson *et al.*, Nucl. Phys. **A661**, 665c (1999).
[13] PHENIX Collaboration, S. White *et al.*, Nucl. Phys. **A698**, 420c (2002).
[14] K. Adcox *et al.*, Phys. Rev. Lett. **86**, 3500 (2001).
[15] K. Adcox *et al.*, Phys. Rev. Lett. **88**, 022301 (2002).
[16] GEANT 3.21, CERN program library.
[17] P. Braun-Munzinger *et al.*, Phys. Lett. B **518**, 41 (2001).
[18] K. Adcox *et al.*, Phys. Rev. Lett. **88**, 242301 (2002).
[19] X. N. Wang and M. Gyulassy, Phys. Rev. D **44**, 3501 (1991).